J. Magn. Soc. Jpn., **47**, 28-37 (2023) <Review>

# Research on spintronic functions of non-metallic materials and its modulation by external fields

M. Shiraishi

Department of Electronic Science and Engineendring, Kyoto University,
*Kyoto-Daigaku-Katsura, Nishikyo-ku, Kyoto 615-8510, Japan.*

Non-metallic materials, such as inorganic/organic semiconductors and topological quantum materials are now collecting significant attention in modern spintronics. The progress of the research field using the materials is quite rapid and tremendous amounts of significant studies have been published. In this review article, some important milestone works are introduced to enhance further acceleration of the research fields.

**Key words:** Organic semiconductors, graphene, inorganic semiconductors, silicon, topological insulator, Weyl ferromagnet, Weyl semimetal, spin injection, spin manipulation, gating effect

## 1. Introduction

Since the discovery of giant magnetoresistance effect, the field of spintronics has been rapidly expanding. As the first-generation material in spintronics, ferromagnetic and nonmagnetic metals have been and is still now playing the central role. Meanwhile, inorganic semiconductors have been collecting significant attention as the second-generation material in spintronics since the advent of diluted ferromagnetic semiconductor and spin transport in semiconductors. In the 21st century, novel materials systems such as organic molecules, hetero-interfaces, atomically flat materials and topological quantum materials are becoming rising stars of materials in spintronics. Attractiveness of non-metallic materials in spintronics is, for example, potential for spin modulation by external fields such as an electric field, long spin coherence and so on. In this review article, significant milestones in spintronics using such non-metallic materials including the author's achievements for the MSJ Award 2022 are introduced, albeit not all of the notable studies cannot be introduced because the field is rapidly expanding, and tremendous amounts of works have been implemented.

## 2. Spintronic function of molecular materials

Attractiveness of molecular materials in spintronics is its small spin-orbit interaction (SOI) attributed to its lightness, which allows expecting good spin coherence. Thus, molecular materials attracted much attention in the beginning of 21st century. In the advent of the research field, magnetoresistance in sexithienyl (T6) [1] and Alq3 [2] were reported by using a conventional electric two-terminal method, of which magnetoresistance (in Alq3) is shown in Fig. 1. Meanwhile, as widely recognized at present, superposition of anisotropic magnetoresistance in an electric local two-terminal method strongly hampers precise detection of spin transport signals, and sufficient elimination of spin-tunneling in molecules was not realized. Furthermore, long-term problems were missing of the Hanle-type spin precession and non-local four-terminal spin transport in most of works using molecules, where both achievements provide steadfast evidence of successful spin transport, albeit a trial to explain the missing was unsuccessfully implemented [3]. The problem also indicates the difficulty in estimating precise spin lifetime in molecules, and most of the works utilized a method of gap-dependence of spin signals instead of the Hanle method. However, to note is that the gap-dependence-like results can be obtained even in spin-dependent tunneling. Since most of molecular materials are low-conductive materials, identification of spin transport mechanisms, i.e., spin injection into molecules or spin-dependent tunneling via molecules, is difficult if spin transport in molecular materials would be successfully realized. Thus, the central research topics of the field with sufficient reliability is an interesting and unique physical feature of spin-dependent tunneling via molecules, where exotic

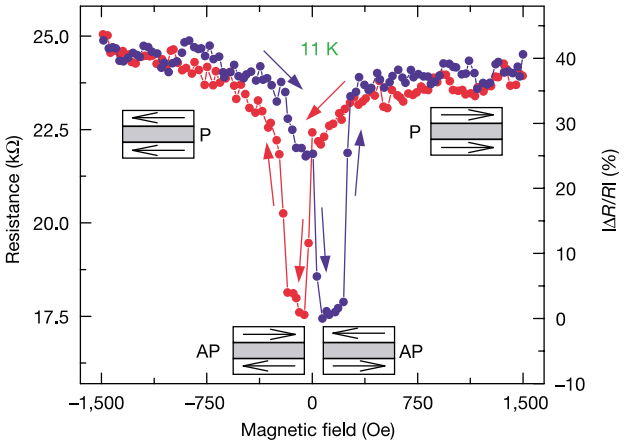


**Fig. 1** Two-terminal magnetoresistance in a Co/Alq3/LaSrMnO spin valve (ref. 2)). Notable is an observation of negative magnetoresistance.

Corresponding author: M. Shiraishi
(e-mail: shiraishi.masashi.4w@kyoto-u.ac.jp).

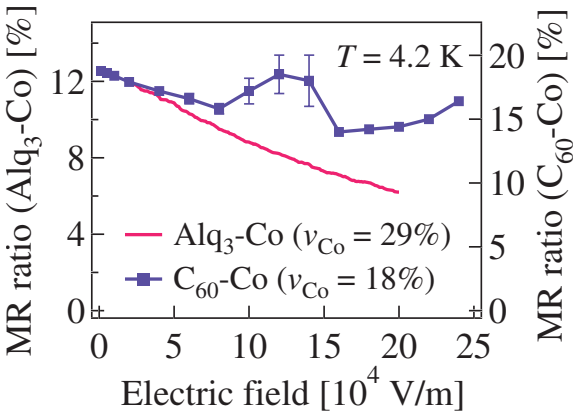


**Fig. 2** Tunnel magnetoresistance in molecule-Co nanocomposite systems (ref. 5)).

enhancement of magnetoresistance ratio was discovered [4-7] (see Fig. 2), until the era of graphene spintronics. Although there were some contributions facing with the remaining serious problems in molecular spintronics [8], lack of serious devotion for solving these problems impedes further progress of the field, and at present, spintronics using molecules except for graphene is unfortunately shrinking. Novel approaches with showing reliable and reproducible evidence are still strongly awaited to help the field from severe stagnation.

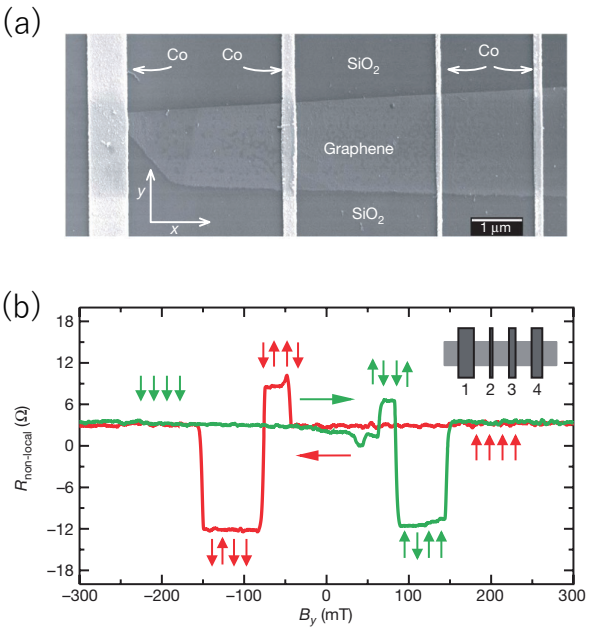


**Fig. 3** Graphene spin valve (left) and observed non-local magnetoresistance at room temperature (right), where the non-local four-terminal measurement technique was introduced (ref. 11)).

Establishment of graphene spintronics strongly helps circumventing the serious stagnation of molecular spintronics. "Discovery" of single-layer graphene (SLG) exhibiting exotic and intriguing topological physics [9,10]

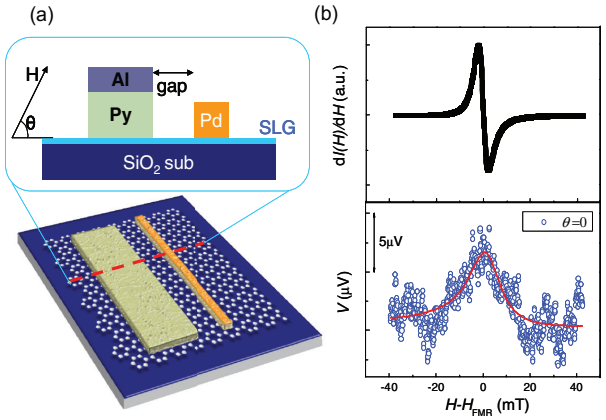


**Fig. 4** (a) Spin transport device using single-layer graphene (SLG), where NiFe (Py) spin source and Pd spin current detector are equipped separately and an external magnetic field is applied to excite ferromagnetic resonance of the Py. (b) The upper panel shows the ferromagnetic resonance spectrum from the Py and the lower panel shows a concomitant electromotive force from the Pd. The external magnetic field is applied at $\theta$ =0. The resonance field is consistent with the field where the peak of the electromotive force appears, which is an evidence of successful spin injection and transport in SLG by spin pumping (ref. 15)).

provided great impact in broad research fields. Quite small effective mass of electrons and holes in SLG enables quite fast charge motion with high mobility and lightness of SLG consisting of only carbon atoms allows good spin coherence, both of which are appropriate physical nature for spin transport. Since 2007, the field of graphene spintronics rapidly expanded, where realization of room temperature spin transport[11,12] by the non-local four-terminal method (Fig. 3), spin lifetime anisotropy/isotropy [13,14], and so forth, and now spin relaxation physics of not only SLG but also bilayer graphene is investigated and understood in detail.

It is also quite notable that graphene spintronics explored an avenue towards van der Waals heterostructure spintronics, where bilayer of SLG and transition metal dichalcogenides (TMDs) is collecting broad attention in view of proximity effect of the SOI.

Notable experimental methods applicable to spin transport measurements for molecular materials are dynamical spin injection. A pioneering work was carried out by using CVD-grown graphene, where room temperature spin transport in SLG was demonstrated in a lateral spin device with separated spin source and detector electrodes (see Fig. 4) [15]. A subsequent achievement of dynamical spin injection into molecule was achieved as polaron spin current transport in conjugated polymer [16] by introducing a vertical spin device for dynamical spin injection and detection in condensed matters [17]. As in semiconductor spintronics, it is corroborated that dynamical spin injection can be a

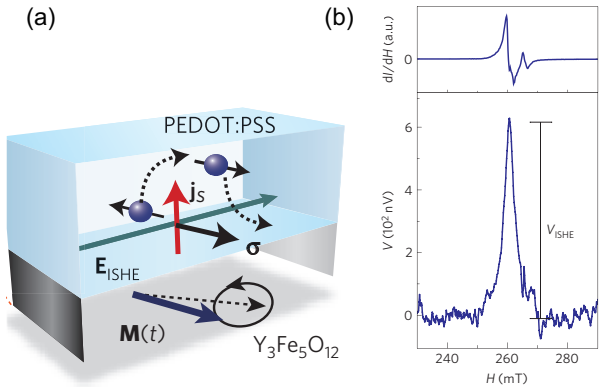


**Fig. 5** (a) Device structure of organic spin convertor. Organic polymer, PEDOT:PSS, is equipped on ferrimagnetic insulator, $Y_3Fe_5O_{12}$ (YIG). (b) The upper panel shows the ferromagnetic resonance spectrum from the YIG and the lower panel shows a concomitant electromotive force from the organic polymer. Again, the magnetic fields where the ferromagnetic resonance and the electromotive force peaks appear are consistent (ref. 18)).

potential approach for injecting spins into molecules. The other notable achievement based on the dynamical spin pumping technique in molecular spintronics is demonstration of spin conversion. As aforementioned, a characteristic nature of molecular materials in spintronics is its weak SOI. Hence, people had been believing that spin charge conversion is impossible in molecules because its SOI is too weak to realize the conversion. The achievement by Ando et al. overturned the conventional understanding (see Fig. 5) [18]. The key for the successful spin conversion in molecules is sufficient spin accumulation by the spin pumping from YIG as the substrate of PEDOT:PSS, a solution-processed spin convertor. Although the conversion efficiency was indeed small, the sufficient spin accumulation into the polymer allows detection of charge flow generated by the inverse spin Hall effect (ISHE). This work opened a new frontier of spin conversion physics, where heavy elements and topological materials played pivotal roles. The same concept was applied for substantiating spin conversion in SLG [19-21], where there was strong debate regarding the mechanisms. The sample structure was the same, SLG/YIG bilayer, in the studies. Mendez et al. claimed that the spin conversion was governed by the Rashba-Edelstein effect due to inversion symmetry breaking along the perpendicular to the SLG plane direction [20]. Meanwhile, our group reported that the ISHE governs the conversion physics by demonstrating ambipolar and gate-modulated spin conversion (see Fig. 6) [21]. The conclusive work was implemented by Raes et al. [14], where spin relaxation in SLG is isotropic resulting in no Rashba field is created in SLG instead of its inversion symmetry breaking along the perpendicular to the plane direction, which unequivocally negated the claim by Mendez et al.

In summary, progress of molecular spintronics is still

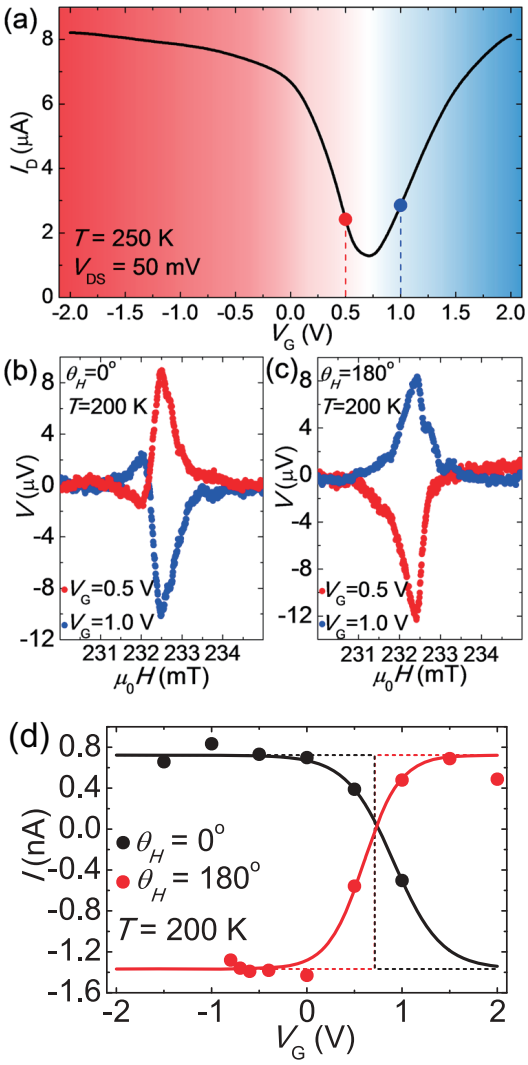


**Fig. 6** (a) Gate voltage dependence of the source-drain electric current in SLG. (b) Gate voltage dependence of electromotive forces in SLG under spin pumping when the carrier is hole (+0.5 V, the red solid line) and electron (+1.0 V, the blue solid line). (c) Gate voltage dependence of the electromotive forces in SLG when the direction of the external magnetic field is reversed. (d) Gate voltage dependence of generated electric current by the ISHE. The saturation of the current under higher gate voltages is compelling evidence that the ISHE, not the Rashba-Edelstein effect, governs the spin conversion (ref. 21)).

lagged of the other spintronics fields and its attractiveness has not been explored yet. Hence, much serious effort is awaited.

### 3. Spintronic function of topological quantum materials

A topological quantum material (TQM) is a novel material phase in 21st century. Since the discovery of the new material phase [22-24], tremendous effort has been made to explore a wide variety of novel and abundant physics appearing in topological insulators (TIs),

topological superconductors (TSCs), Weyl semimetals and Weyl ferromagnets for creating novel electric and spintronics devices by utilizing their fast carrier mobilities due to the linear band structures. Contrary to topologically trivial materials, TQMs exhibit great potential to show exotic and intriguing physical properties. TIs possess spin-polarized Dirac fermion bands resulting in the quantum spin Hall effect and persistent spin current that are resilient to defects [25], and TSCs can be a material platform for realizing fault-tolerant quantum computing utilizing Majorana fermions that can exist in TSC states [26]. A Weyl semimetal is a considerably new family of TQMs [27], where nondegenerate linear conduction and valence bands touch each other at the Weyl point by breaking either spatial or time reversal symmetries, yielding gapless Weyl fermions. In addition, a Weyl semimetal is known to be an ideal material platform of the appearance of the Adler-Bell-Jackiw (ABJ) anomaly of Weyl fermions [28], which is due to the breaking of chiral symmetry in massless Weyl fermions under quantum fluctuation. The ABJ anomaly was experimentally corroborated in TaAs, NbAs, TaP and $WTe_2$ [29-32] and is the fingerprint of the Weyl nature. A Weyl ferromagnet and anti-ferromagnet are also a novel family of TQMs, where $Co_2MnGa$ [33] and $Mn_3Sn$ [34] are representative materials, respectively, and a number of spin-related effects, such as giant anomalous Hall [35,36] and Nernst effects [35], giant spin-Hall and inverse spin-Hall effects [37] in $Co_2MnGa$ and the magnetic spin Hall effect ( a novel family of Hall effects) [38] in $Mn_3Sn$, has been discovered and detected. Because tremendous amounts of works have been implemented, it is difficult to cover and follow the whole research topics for TQMs, the author introduces his own and related works regarding spin polarization detection in this chapter.

As aforementioned, topologically-protected surface spin polarization in TIs is an intriguing research object in spintronics, and much effort was paid for detecting the spin polarization. Two possible pathways to the goal; a potentiometric method and a spin pumping method. The first study to claim the detection of the surface spin polarization was implemented by using $Bi_2Se_3$, a three-dimensional TI [39], where the potentiometric method was utilized. However, strong debate arose about what the authors detected, because the Fermi level of $Bi_2Se_3$ is located in the conduction band and the topological state is buried into the topologically trivial bulk state. Thus, a question that the authors detected spin polarization attributed not to the topological state but to the Rashba state. The similar debate also arose to the claim of the room temperature detection of the topological surface state in $Bi_2Se_3$. To avoid such confusion, identification of the polarity of the spin signals, which comes from the spin alignments of the surface spin current of a TI and detector ferromagnet, is quite significant [40], and control experiments to support a claim is indispensable. Thus, comparison of results in a bulk non-insulative TI (such as

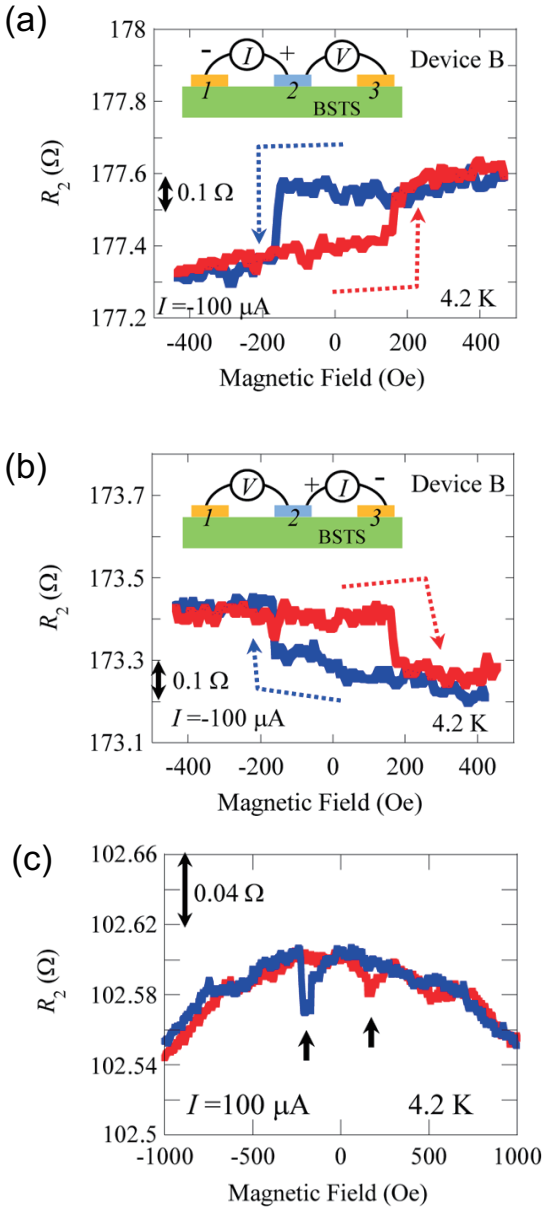


**Fig. 7** (a) Magnetoresistance due to the topologically-protected surface spin polarization in BiSbTeSe at 4.2 K. (b) Magnetoresistance in BiSbTeSe when the direction of the charge flow was reversed. Polarity of the magnetoresistance was opposite to that in (a). (c) Missing magnetoresistance in BiSe at 4.2 K, which signifies the position of the Fermi level is crucial for successful detection of the surface spin polarization in topological insulator (ref. 41)).

$Bi_2Se_3$) and a bulk insulative TI (such as $Bi_{1.5}Sb_{0.5}Te_{1.7}Se_{0.3}$) is quite important. Indeed, the authors' group introduced $Bi_{1.5}Sb_{0.5}Te_{1.7}Se_{0.3}$ as a possible candidate TI and reported successful detection of the surface spin polarization up to ca. 150 K (Fig. 7) [41]. The spin signal is detectable only from $Bi_{1.5}Sb_{0.5}Te_{1.7}Se_{0.3}$ and no signal is observed in $Bi_2Se_3$ even at 4 K, which is compelling evidence that the detected spin signal is

ascribed to the topologically-protected surface helical spin state. To note is that the similar comparison was carried out in the spin pumping approach [42].

Topological nature in TQMs allows the other intriguing physics in Weyl materials. TaAs is the first material as a Weyl material [43], and a Weyl material collects significant attention because of its band-crossing points that give rise to plenty of unique physical properties, such as the Fermi arc surface states, the chiral anomaly coming from the Nielsen-Ninomiya theorem [44] and monopole-like Berry curvature [45]. In addition, a prominent class of Weyl semimetals is Weyl magnetic materials such as ferromagnetic $Co_2MnGa$ and antiferromagnetic $Mn_3Sn$. These two materials are playing pivotal roles in condensed-matter physics because of the recent discoveries of the gigantic anomalous Hall effect (AHE) [46,47], the magnetic spin Hall effect (a novel family of Hall effects) [48], and spin caloritronics phenomena such as the large anomalous Nernst effect [49,50]. Additionally, magnetic Heusler alloys have emerged as promising materials in the field of spintronics due to their either half-metallic or semimetallic nature, which would lead to a high spin polarization [51,52], as has been reported in Co-based full Heusler compounds [53,54]. $Co_2MnGa$ is a representative Weyl ferromagnet as aforementioned, and sizable spin Hall effect (SHE) and ISHE can be expected due to its topological nature like in the case of AHE. Indeed, coexistence of the giant ISHE and the SHE was corroborated by using the electric non-local four-terminal method [55] and more importantly, it was observed that Onsager's reciprocity does not hold for the system unlike for conventional metallic ferromagnets (see Fig. 8) [56]. Furthermore, two orders of magnitude enhancement of magnetoresistance attributed to the anomalous Nernst effect in single $Co_2MnGa$ wire was also reported [57].

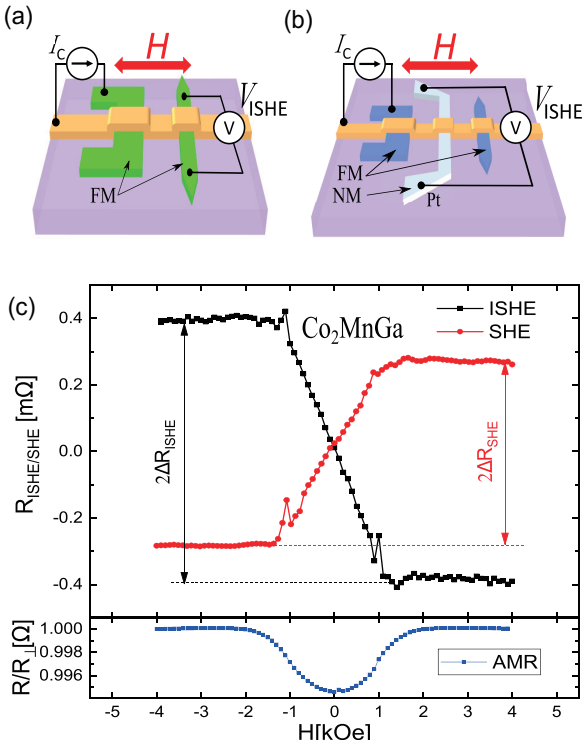


**Fig. 8** Measuring setups for the ISHE (a) and the SHE (b) in $Co_2MnGa$, a Weyl ferromagnet. (c) Spin resistances due to the ISHE and the SHE, where Onsager reciprocity is broken (ref. 55)).

Not only Weyl ferromagnets and antiferromagnets, but a Weyl semimetal also enable significant spintronic effects. Among a number of Weyl semimetals, the $T_d$-type $WTe_2$ [58] possesses abundant spintronic nature, where the Weyl points appear at the crossing of the oblique conduction and valence bands due to the broken inversion symmetry and nonsaturating giant positive magnetoresistance is a manifestation of the type-II Weyl character [59,60]. As aforementioned, fictitious magnetic monopoles can appear at each Weyl point, which gives rise to in-plane spin polarization at the surface of the Weyl semimetal [61,62]. In fact, the in-plane spin polarization along the *b*-axis ($S_y$, parallel to the $WTe_2$ plane) is ascribed to the Weyl node, which was electrically detected [63]. Meanwhile, the $S_y$ polarization disappears at very low temperature (< 15 K) due to lattice expansion, which has been hampering spin information propagation and extraction at higher temperature available for all-electric spin devices. Importantly, angle-resolved photoemission spectroscopy (ARPES) revealed other possible spin polarizations along the *c*-axis ($S_z$, perpendicular to the plane) in addition to those along the *b*-axis in $WTe_2$ [64]. A pioneering work utilizing the $S_z$ polarization of $WTe_2$ is detection of anomalous spin torque in ST-FMR (see Fig. 9) [65,66]. The authors introduced a potentiometric approach to create and detect the $S_z$ polarization, and experimentally proved that the $S_z$ polarization is quite resilient to thermal

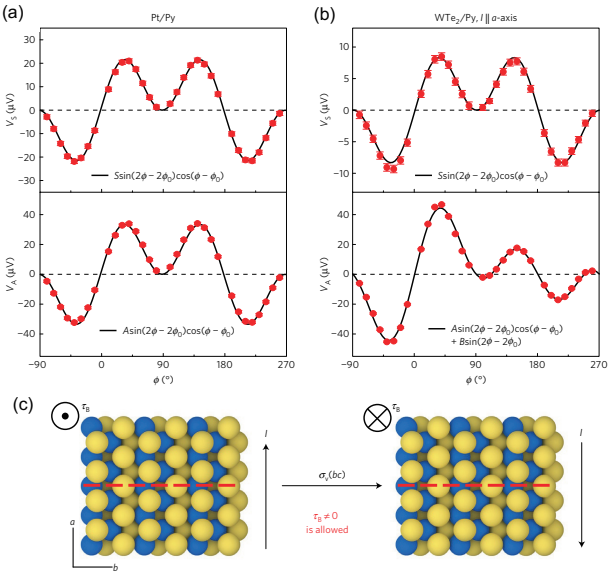


**Fig. 9** Anomalous spin-orbit torque (SOT) appearing in $T_d$-type $WTe_2$. (a) SOT in Pt/Py and (b) SOT in $WTe_2$/Py, where the electric current flows along the *a*-axis. (c) Schematic images of structural symmetry breaking in $WTe_2$ (ref. 65)).

fluctuation and spin signals are detectable up to RT [67], which enables creation of all-electric spin devices using a Weyl semimetal (Fig. 10).

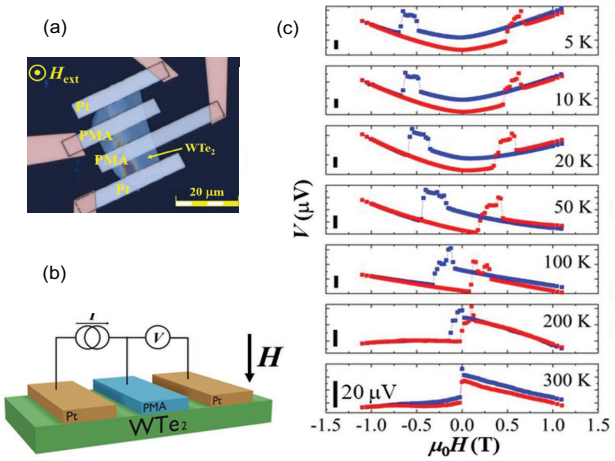


**Fig. 10** (a) Optical microscopic view of an all-electric spin device using $T_d$-type $WTe_2$, a Weyl semimetal. (b) Measuring setup for the $S_z$ spin polarization detection created in the $WTe_2$. (c) Temperature dependence of magnetoresistance of the $WTe_2$ spin device. The $S_z$ spin polarization is attributed to structural symmetry breaking along the $b$-axis in $WTe_2$ and is resilient to thermal fluctuation (ref. 67)).

In summary, horizon of topological spintronics is expanding rapidly, and a number of experimental approaches allows investigating significant and attractive topological nature in TQMs in spintronic viewpoints.

### 4. Spintronic function of inorganic semiconductors

For several decades, inorganic semiconductors play one of central roles in material choice in spintronics. There are two pivotal trends in inorganic semiconductor spintronics: (1) diluted magnetic semiconductors, and (2) spin transport in semiconductors. Regarding the first topic, epoch-making achievements, such as electric-field control of ferromagnetism in InMnAs [68] and realization of RT ferromagnetism in InFeAs [69] since the first realization of diluted magnetic semiconductor [70]. Meanwhile, unfortunately, the author has not been focusing his work on the material, and in this chapter, the author sheds light only on spin transport in inorganic semiconductor, especially group-IV inorganic semiconductors.

Spin injection, transport, detection and manipulation in inorganic semiconductor are key scientific issues for applications towards spin-based transistors. In principle, two different types of spin transistors using inorganic semiconductors are: (1) Das-Datta type [71] and (2) Sugahara-Tanaka type [72]. In addition, the Sugahara-Tanaka type spin transistor allows a new spin logic system, the Dery-Sham type spin logic [73]. To note is that compound inorganic semiconductors such as III-V

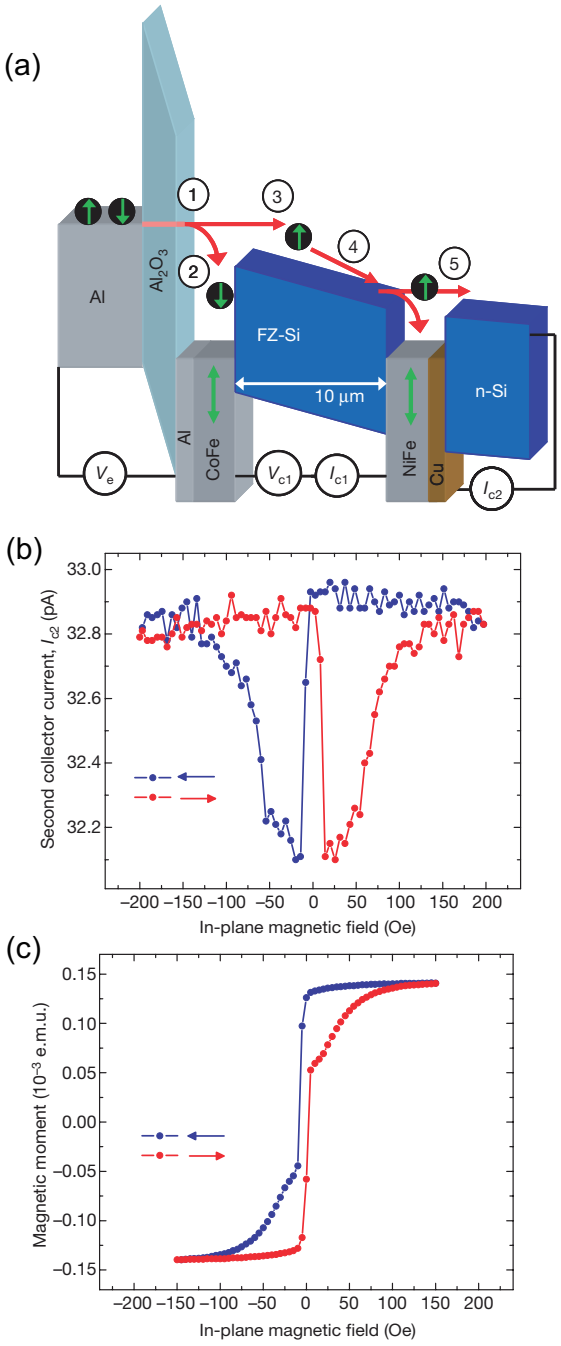


**Fig. 11** (a) Schematic image of Si-based hot-electron transistor. (b) Magnetoresistance effect due to spin injection and spin transport via 10 mm non-doped Si. (c) Magnetization curves of the CoFe electrode (ref. 74)).

semiconductors are available to the Das-Datta type and group IV inorganic semiconductors including graphene are suitable for the Sugahara-Tanaka type, since operation principles of both transistors are different. Group-IV semiconductors (diamond, Si and Ge) possess lattice inversion symmetry and carbon and Si are light elements, which is the underlying physics of possible long spin coherence in the materials, such as graphene and Si, and is the reason why these materials garner much

attention. In fact, graphene exhibits long-range spin transport over 10 mm, whereas spin lifetime in graphene is merely about tens picoseconds mainly due to its large Fermi velocity originating from the Dirac nature of graphene. Si exhibits long spin lifetime over several nanoseconds and relatively long spin diffusion length of over 1 mm, i.e., long spin lifetime and diffusion length successfully coexist.

The chronicle of Si spintronics substantially started from hot-electron spin injection into non-doped Si (Fig. 11) [74], although some challenging but unsuccessful works using some different approaches had been reported before. The authors of ref. 74 introduced a hot-electron transistor structure, where the wafer bonding technique was used, and realized spin injection up to 260 K [75], long-range spin transport of 2 mm [76], and multiple spin precession of 13p due to the Hanle effect [77]. The notable is that this approach elaborately circumvents the reliability problem of the electric two-terminal method as partly described in Chap. 2. These achievements manifested great spintronic potential of Si and greatly stimulated researchers in semiconductor spintronics. Meanwhile, since the hot-electron transistor structure was used, the output spin signal was considerably small to be an order of picoampere and modulation of spin signal by gating was difficult, which can strongly hinder practical application of Si-based spin devices. Thus, reliable and reproducibly spin injection and transport in Si by the other approach available for spin transistors. The authors introduced the electric non-local four-terminal method to achieve successful spin injection and creation of pure spin current in Si [78], and room temperature spin injection/transport/detection in n-type degenerate Si with Hanle-type spin precession was achieved (see Fig. 12) [79]. Furthermore, spin injection/transport/detection in non-degenerate n-type Si and subsequent spin signal modulation by gating were achieved at room temperature [80,81], where the on/off ratio was enhanced >$10^4$ (Fig. 13) [81]. In the course of these significant studies, a number of detailed spintronic physics in Si were clarified: spin drift in Si

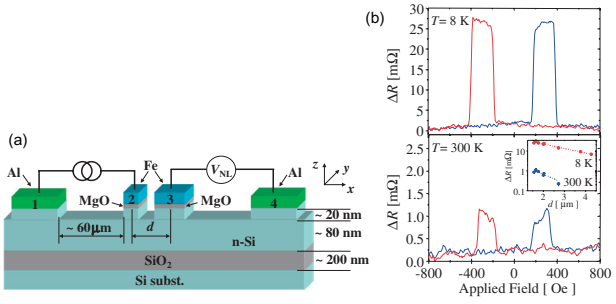


**Fig. 12** (a) Schematic image of a four-terminal degenerate n-type Si spin valve. (b) Non-local magnetoresistance in the Si spin valve at 8 K (the upper panel) and 300 K (the lower panel). The inset of the lower panel shows gap-length dependence of spin resistances (ref. 79)).

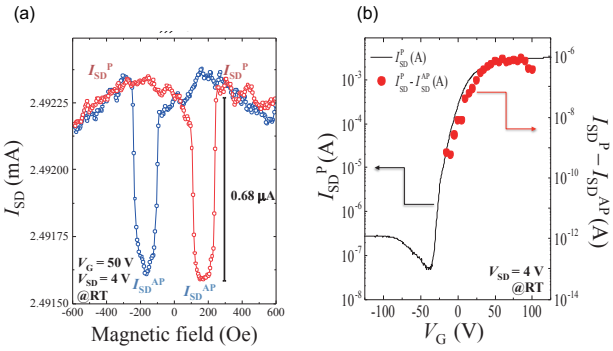


**Fig. 13** (a) Magnetoresistance in spin-dependent electric current of non-degenerate n-type spin MOSFET at room temperature. (b) Gate voltage dependence of the source-drain current (the black solid line) and spin signals (the red closed circles) (ref. 81)).

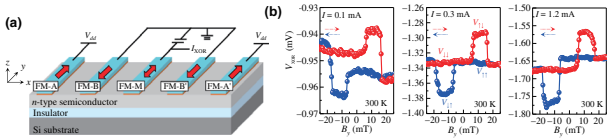


**Fig. 14** (a) Spin logic circuit made of Si spin MOSFET. (b) An example XOR logic operation of the Si spin logic. For detail, see ref. 94).

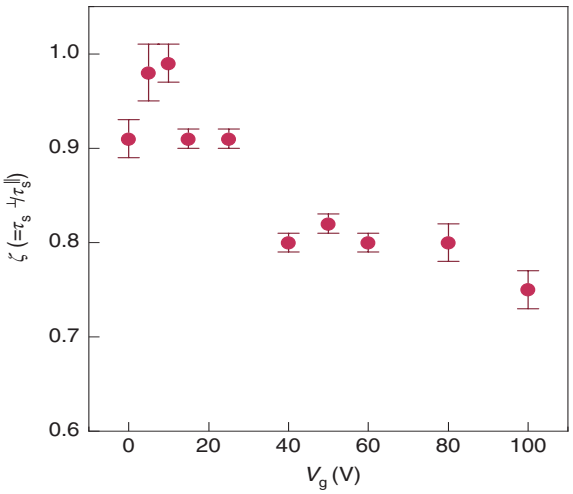


**Fig. 15** Spin lifetime anisotropy in in-plane and perpendicular-to-the-plane spins in Si spin MOSFET as a function of gate voltages. The anisotropy exists without a gate voltage due to the built-in Rashba field in the Si channel, and the anisotropy is once suppressed by the gate voltage application (ref. 96)).

[82,83], bias voltage dependence of spin signals [84], clarification of the origin the "inverted Hanle" effect [85], enhancement of spin signals by utilizing spin drift and clarification of its underlying physics [86-88], achievement of thermal spin injection in Si [89], investigation of gating effects on spin signals [90], and thermal annealing effects on spin signals [91,92]. Notable achievements in Si spintronics from application-oriented viewpoints are

demonstration of over 1% magnetoresistance ratio [93] and spin logic operation (Fig. 14) [94]. Furthermore, significant achievements in basic physics viewpoints are spin-pumping-induced spin transport in p-type Si [95] and electric field modulation of spin precession (spin manipulation without an external magnetic field) due to synthetic Rashba field in $Si/SiO_2$ [96]. Especially, spin manipulation by the gate electric field in Si spin FET shown in Fig. 15 counters conventional understandings that the SOI in Si is negligibly small and the Rashba field does not play a dominant role in Si. The achievement can be regarded as one of subsequent studies that gate control of SOI, resulting in the ISHE, in ultrathin metallic films [97-99]. It is also noted that spin transport in the other group-IV semiconductor, Ge, was also achieved at room temperature by spin pumping [100], which enables subsequent studies using Ge towards spin transistor creation [101,102].

In summary, inorganic semiconductors are playing one of pivotal roles in spintronics, and its research field expands to both application-oriented and fundamental directions. Especially, group-IV semiconductors such as Si and Ge (and in addition, graphene and diamond) play an important role in the field.

**Acknowledgements** The author is indebted to all collaborators, especially Prof. Yoshishige Suzuki and his group members in Osaka University, and Dr. Tomoyuki Sasaki, Mr. Hayato Koike and group members in TDK corporation. He also acknowledges to his colleagues and students of his group in Osaka University (2010-2013) and Kyoto University (2013-) especially Dr. Eiji Shikoh, Dr. Yuichiro Ando, Dr. Ryo Ohshima, Dr. Ei Shigematsu and Dr. Eiiti Tamura, for their strong and supportive collaboration. Financial supports from the Ministry of Education, Culture, Sports, Science and Technology of Japan and the Japan Science and Technology Agency are deeply appreciated.

## References

1) V.A. Dediu, M. Murgia, F.C. Matacotta, C. Taliani and S. Barbaner: *Solid State Commun.* **122**, 181 (2002).
2) Z. Xiong, D. Wu, Z. Valy Vardeny and J. Shi: *Nature* **427**, 821 (2004).
3) P.A. Bobbert, W. Wagemans, F.W.A. van Oost, B. Koopmans and M. Wohlgenannt: *Phys. Rev. Lett.* **102**, 156604 (2009).
4) S. Miwa, M. Shiraishi, M. Mizuguchi, T. Shinjo and Y. Suzuki: *Jpn. J. Appl. Phys.* **45**, L717 (2006).
5) S. Miwa, M. Shiraishi, S. Tanabe, M. Mizuguchi, T. Shinjo and M. Shiraishi: *Phys. Rev. B***76**, 214414 (2007).
6) D. Hatanaka, S. Tanabe, H. Kusai, R. Nouchi, T. Nozaki, T. Shinjo, Y. Suzuki, H. Wan, K. Takanashi and M. Shiraishi: *Phys. Rev. B***79**, 235402 (2009).
7) Y. Sakai, E. Tamura, S. Toyokawa, E. Shikoh, V.K. Lazarov, A. Hirohata, T. Shinjo, Y. Suzuki and M. Shiraishi: *Adv. Func. Mater.* **22**, 3845 (2012).
8) "A better spin on organic semiconductors" (editorials): *Nature Nanotech.* **8**, 611 (2013).
9) K.S. Novoselov, A.K. Geim, S.V. Morozov, D. Jiang, M.I. Latsnelson, I.V. Grigorieva, S.V. Dubonos and A.A. Firsov: *Nature* **438**, 197 (2005).
10) Y. Zhang, Y-W. Tan, H.L. Stormer and P. Kim: *Nature* **438**, 201 (2005).
11) N. Tombros, C. Jozsa, M. Popinciuc, H.T. Jonkman and B.J. van Wees: *Nature* **448**, 571 (2007).
12) M. Ohishi, M. Shiraishi, R. Nouchi, T. Nozaki, T. Shinjo and Y. Suzuki: *Jpn. J. Appl. Phys.* **46**, L605 (2007).
13) N. Tombros, S. Tanabe, A. Veligura, C. Jozsa, M. Popinciuc, H.T. Jonkman and B.J. van Wees: *Phys. Rev. Lett.* **101**, 046601 (2008).
14) B. Raes, J.E. Scheerder, M.V. Costache, F. Bonell, J.F. Sierra, J. Cuppens, J. Van de Vondel and S.O. Valenzuela: *Nature Commun.* **7**, 11444 (016).
15) Z. Tang, E. Shikoh, H. Ago, K. Kawahara, Y. Ando, T. Shinjo and M. Shiraishi: *Phys. Rev. B***87**, 140401(R) (2013).
16) S. Watanabe, K. Ando, K. Kang, S. Mooser, Y. Vaynzof, H. Kurebayashi, E. Saitoh and H. Sirringhaus: *Nature Phys.* **10**, 308 (2014).
17) Y. Kitamura, E. Shikoh, Y. Ando, T. Shinjo and M. Shiraishi: *Sci. Reports* **3**, 1739 (2012).
18) K. Ando, S. Watanabe, S. Mooser, E. Saitoh and H. Sirringhaus: *Nature Mater.* **12**, 622 (2013).
19) R. Ohshima, A. Sakai, Y. Ando, T. Shinjo, K. Kawahara, H. Ago and M. Shiraishi: *Appl. Phys. Lett.* **105**, 162401 (2014).
20) J.B.S. Mendes, O. Alves Santos, L.M. Mireles, R.G. Lacerda, L.H. Viela-leao, F.L.A. Machado, R.L. Rodriguez-Suarez, A. Azevedo and S.M. Rezende: *Phys. Rev. Lett.* **115**, 226601 (2015).
21) S. Dushenko, H. Ago, K. Kawahara, T. Tsuda, S. Kuwabata, T. Takenobu, T. Shinjo, Y. Ando and M. Shiraishi: *Phys. Rev. Lett.* **116**, 166102 (2016).
22) M.Z. Hasan and C.L. Kane: *Rev. Mod. Phys.* **82**, 3045-3067 (2010).
23) Z.-L. Qi and S.-C. Zhang: *Rev. Mod. Phys.* **83**, 1057-1110 (2011).
24) N.P. Armitage, E.J. Mele and A. Vishwanath: *Rev. Mod. Phys.* **90**, 015001 (2018).
25) C.L. Kane and E.J. Mele: *Phys. Rev. Lett.* **95**, 226801 (2005).
26) M. Sato and S. Fujimoto: *J. Phys. Soc.* Jpn. **85**, 072001 (2016).
27) S. Murakami: *New J. Phys.* **9**, 356 (2007).
28) H.B. Nielsen and M. Ninoymiya: *Phys. Lett. B***130**, 389 (1983).
29) C.-L. Zhang et al.: *Nat. Commun.* **7**, 10735 (2016).
30) X.C. Huang et al.: *Phys. Rev. X* **5**, 031023 (2015).
31) F. Arnold et al.: *Nat. Commun.* **7**, 11615 (2016).
32) Y-Y. Lv et al.: *Phys. Rev. Lett.* **118**, 096603 (2017).
33) I. Belopolski, K. Manna, D.S. Sanchez, G. Chang, B. Ernst, J. Yin, S.S. Zhang, Y. Cochran, N. Shumiya, M. Z. Hasan: *Science* **365**, 1278 (2019).
34) K. Kuroda, T. Tomita, M.-T. Suzuki, C. Bareille, A. A. Nugroho, P. Goswami, M. Ochi, M. Ikhlas, M. Nakayama, S. Akebi, R. Noguchi, R. Ishii, N. Inami, K. Ono, K. Kumigashira, A. Varykhalov, T. Muro, T. Koretsune, R. Arita, S. Shin, Takeshi Kondo, and S. Nakatsuji: *Nature Mater.* **16**, 1090 (2017).
35) A. Sakai, Y. P. Mizuta, A. A. Nugroho, R. Sihombing, T. Koretsune, M.-T. Suzuki, N. Takemori, R. Ishii, D. Nishio-Hamane, R. Arita, P. Goswami, and S. Nakatsuji: *Nature Phys.* **14**, 1119 (2018).
36) G. Chang, S. Y. Xu, X. Zhou, S. M. Huang, B. Singh, B. Wang, I. Belopolski, J. Yin, S. Zhang, A. Bansil, H. Lin, and M. Z. Hasan: *Phys. Rev. Lett.* **119**, 156401 (2017).
37) L. Leiva, S. Granville, Y. Zhang, S. Dushenko, E. Shigematsu, T. Shinjo, R. Ohshima, Y. Ando and M. Shiraishi: *Phys. Rev. B***103**, L041114 (2021).
38) M. Kimata, H. Chen, K. Kondou, S. Sugimoto, P. K. Muduli, M. Ikhlas, Y. Omori, T. Tomita, A. H. MacDonald, S. Nakatsuji, and Y. Otani: *Nature* **565**, 627 (2019).
39) C. Li, O.M. van't Erve, J.T. Robinson, Y. Liu, L. Li, B.T.

Jonker: *Nat. Nanotech.* **9**, 218 (2014).
40) E.K. de Vries, A.M. Kamerbeck, N. Koirala, M. Brahlek, M. Salehi, S. Oh, B.J. van Wees and T. Banerjee: *Phys. Rev. B* **92**, 201102(R) (2015).
41) Yu. Ando, T. Hamasaki, T. Kurokawa, K. Ichiba, F. Yang, M. Noval, S. Sasaki, K. Segawa, Yo. Ando and M. Shiraishi: *Nano Lett.* **14**, 6226 (2014).
42) Y. Shiomi, K. Nomura, Y. Kajiwara, K. Eto, M. Novak, K. Segawa, Yo. Ando and E. Saitoh: *Phys. Rev. Lett.* **113**, 196601 (2014).
43) B.Q. Lv et al.: *Phys. Rev. X* **5**, 031013 (2015).
44) H. Nielsen and M. Ninomiya, Phys. Lett. B **130**, 389 (1983).
45) H. Yang, Y. Sun, Y. Zhang, W.-J.Shi, S.S. Parkin and B. Yan: *New J. Phys.* **19**, 015008 (2017).
46) A. Sakai et al.: *Nature Phys.* **14**, 1119 (2018).
47) G. Chang et al.: *Phys. Rev. Lett.* **119**, 156401 (2017).
48) M. Matsuda, N. Kanda, T. Higo, N. Armitage, S. Nakatsuji and R. Matsunaga: *Nature Commun.* **11**, 909 (2020).
49) B.M. Ludbrook, B.J. Ruch and S. Granville: *Appl. Phys. Lett.* **110** 062408 (2017).
50) S. Kanatsuji, N. Kiyohara and T. Higo: *Nature* **527**, 212 (2015).
51) H. Reichlova et al.: *Appl. Phys. Lett.* **113**, 212405 (2018).
52) J.M.D. Coery and M. Venkatesam: *J. Appl. Phys.* **91**, 8345 (2002).
53) C. Felser and G.H. Hecher: *Spintronics: From Materials to Devices* (Springer, Dordrecht, Heidelberg, New York, London, 2013).
54) T. Kimura, N. Hashimoto, S. Yamada, M. Miyao and K. Hamaya: *NPG Asia Mater.* **4**, e9 (2012).
55) L. Leiva, S. Granville, Y. Zhang, S. Dushenko, E. Shigematsu, T. Shinjo, R. Ohshima, Y. Ando and M. Shiraishi: *Phys. Rev. B* **103**, L041114 (2021).
56) Y. Omori, E. Sagasta, Y. Niimi, M. Gradhand, L.E. Hueso, F. Casanova and Y. Otani: *Phys. Rev. B* **99**, 014403 (2019).
57) L. Leiva, S. Granville, Y. Zhang, S. Dushenko, E. Shigematsu, T. Shinjo, R. Ohshima, Y. Ando and M. Shiraishi: *Phys. Rev. Materials* **6**, 064201 (2022).
58) A.A. Soluyanov, D. Gresch, Z. Wang, Q. Wu, M. Troyer, X. Dai, B.A. Bernevig: *Nature* **527**, 495 (2015).
59) M.N. Ali, J. Xiong, S. Flynn, J. Tao, Q.D. Gibson, L.M. Schoop, T. Liang, N. Haldolaarachchige, M. Hirschberger, N.P. Ong, R.J. Cava: *Nature* 514, 205 (2014).
60) Y. Qi et al.: *Nat. Commun.* **7**, 11038 (2015).
61) H.B. Nielsen, M. Ninomiya: *Nucl. Phys. B* **185**, 20 (1981).
62) H.B. Nielsen, M. Ninomiya: *Nucl. Phys. B* **193**, 173 (1981).
63) P. Li, W. Wu, Y. Wen, C. Zhang, J. Zhang, S. Zhang, Z.Yu, S.A. Yang, A. Manchon, X-x. Zhang: *Nat. Commun.* **9**, 3990 (2018).
64) P.K. Das, D.D. Sante, I. Vobornk, J. Fujii, T. Okuda, E. Bruyer, A. Gyenis, B.E. Feldman, J. Tao, R. Ciancio, G. Rossi, M.N. Ali, S. Picozzi, A. Yazdani, G. Panaccione, R.J. Cava: *Nat. Commun.* **7**, 10847 (2016).
65) D. MacNeil, G.M. Stiehl, M.H.D. Guimaraes, R.A. Buhrman, J. Park, D.C. Ralph: *Nat. Phys.* **13**, 300 (2017).
66) D. MacNeil, G.M. Stiehl, M.H.D. Guimaraes, N.D. Reynolds, R.A. Buhrman, D.C. Ralph: *Phys. Rev. B* **96**, 054450 (2017).
67) K. Ohnishi, M. Aoki, R. Ohshima, E. Shigematsu, Y. Ando, T. Takenobu and M. Shiraishi: *Adv. Electron. Mater.* **8**, 2200647 (2022).
68) H. Ohno, D. Chiba, F. Matsukura, T. Omiya, E. Abe, T. Dietl, Y. Ohno and K. Ohtani: *Nature* **408**, 944 (2000).
69) L.D. Anh, P.N. Hai and M. Tanaka: *Nature Commun.* **7**, 13810 (2016).
70) H. Ohno, H. Munekata, T. Penney, S. von Molnar and L.L. Chang: *Phys. Rev. Lett.* **68**, 2664 (1992).
71) S. Datta and B. Das: *Appl. Phys. Lett.* **56**, 665 (1990).
72) S. Sugahara and M. Tanaka: *Appl. Phys. Lett.* **84**, 2307 (2004).
73) H. Dery, P. Dalal, L. Cywinski and L.J. Sham: *Nature* **447**, 573 (2007).
74) I. Appelbaum, B. Haung and D.J. Monsma: *Nature* **447** ,295 (2007).
75) B. Huang, H-J. Jang and I. Appelbaum: *Appl. Phys. Lett.* **93**, 162508 (2008).
76) Y. Lu and I. Appelbaum: *Appl. Phys. Lett.* **97**, 162501 (2010).
77) B. Huang, D.J. Monsma and I. Appelbaum: *Phys. Rev. Lett.* **99**, 177209 (2007).
78) T. Sasaki, T. Oikawa, T. Suzuki, M. Shiraishi, Y. Suzuki and K. Tagami: *Appl. Phys. Express* **2**, 053003 (2009).
79) T. Suzuki, T. Sasaki, T. Oikawa, M. Shiraishi, Y. Suzuki and K. Noguchi: *Appl. Phys. Express* **4**, 023003 (2011).
80) T. Sasaki, Y. Ando, M. Kameno, T. Tahara, H. Koike, T. Oikawa, T. Suzuki and M. Shiraishi: *Phys. Rev. Applied* **2**, 034005 (2014).
81) T. Tahara, H. Koike, M. Kameno, T. Sasaki, Y. Ando, K. Tanaka, S. Miwa, Y. Suzuki and M. Shiraishi: *Appl. Phys. Express* **8**, 113004 (2015).
82) M. Kameno et al.: *Appl. Phys. Lett.* **101**, 122413 (2012).
83) M. Kameno et al.: *Appl. Phys. Lett.* **104**, 092409 (2014).
84) M. Shiraishi, Y. Honda, E. Shikoh, Y. Suzuki, T. Shinjo, T. Sasaki, T. Oikawa, K Noguchi and T. Suzuki: *Phys. Rev. B* **83**, 241204(R) (2011).
85) Y. Aoki, M. Kameno, Y. Ando, E. Shikoh, Y. Suzuki, T. Shinjo, M. Shiraishi, T. Sasaki, T. Oikawa and T. Suzuki: *Phys. Rev. B* **86**, 081201(R) (2012).
86) T. Sasaki, T. Suzuki, Y. Ando, H. Koike, T. Oikawa, Y. Suzuki and M. Shiraishi: *Appl. Phys. Lett.* **104**, 052404 (2014).
87) T. Tahara, Y. Ando, M. Kameno, H. Koike, K. Tanaka, S. Miwa, Y. Suzuki, T. Sasaki, T. Oikawa and M. Shiraishi: *Phys. Rev. B* **93**, 214406 (2016).
88) S. Lee, F. Rortais, R. Ohshima. Y. Ando, S. Miwa, Y. Suzuki, H. Koike and M. Shiraishi: *Phys. Rev. B* **99**, 064408 (2019).
89) N. Yamashita, Y. Ando, H. Koike, S. Miwa, Y. Suzuki and M. Shiraishi: Phys. Rev. Applied **9**, 054002 (2018).
90) S. Lee, F. Rortais, R. Ohshima. Y. Ando, M. Goto, S. Miwa, Y. Suzuki, H. Koike and M. Shiraishi: *Appl. Phys. Lett.* **116**, 022403 (2020).
91) N. Yamashita, S. Lee, R. Ohshima, E. Shigematsu, H. Koike, Y. Suzuki, S. Miwa, M. Goto, Y. Ando and M. Shiraishi: *AIP Adv.* **10**, 095021 (2020).
92) N. Yamashita, S. Lee, R. Ohshima, E. Shigematsu, H. Koike, Y. Suzuki, S. Miwa, M. Goto, Y. Ando and M. Shiraishi: *Sci. Reports* **11**, 10583 (2021).
93) H. Koike, S. Lee, R. Ohshima, E. Shigematsu, M. Goto, S. Miwa, Y. Suzuki, T. Sasaki, Y. Ando and M. Shiraishi: *Appl. Phys. Express* **13**, 083002 (2020).
94) R. Ishihara, Y. Ando, S. Lee, R. Ohshima, M. Goto, S. Miwa, Y. Suzuki, H. Koike and M. Shiraishi: *Phys. Rev. Applied* **13**, 044010 (2020).
95) E. Shikoh, K. Ando, K. Kubo, E. Saitoh, T. Shinjo and M. Shiraishi: *Phys. Rev. Lett.* **110**, 127201 (2013).
96) S. Lee, H. Koike, M. Goto, S. Miwa, Y. Suzuki, N. Yamashita, R. Ohshima, E. Shigematsu, Y. Ando and M. Shiraishi: *Nature Mater.* **20**, 1228 (2021).
97) S. Dushenko, M. Hokazono, K. Nakamura, Y. Ando, T. Shinjo and M. Shiraishi: *Nature Commun.* **9**, 3118 (2018).
98) S. Yoshitake, R. Ohshima, T. Shinjo, Y. Ando and M. Shiraishi: *Appl. Phys. Lett.* **117**, 092406 (2020).
99) R. Ohshima, Y. Kohsaka, Y. Ando, T. Shinjo and M. Shiraishi: *Sci. Reports* **11**, 21799 (2021).
100) S. Dushenko, M. Koike, Y. Ando, T. Shinjo, M. Myronov and M. Shiraishi: *Phys. Rev. Lett.* **114**, 196602 (2015).
101) A. Yamada, M. Yamada, M. Honda, S. Yamada, K. Sawano and K. Hamaya: *Appl. Phys. Lett.* **119**, 192404 (2021).
102) M. Yamada, F. Kuroda, M. Tsukahara, S. Yamada,

T. Fukushima, K. Sawano, T. Oguchi and K. Hamaya: *NPG Asia Mater.* **12**, 47 (2020).

**Received Nov. 17, 2022; Accepted Dec. 14, 2022.**